Both chemotaxis and net motility greatly influence the infectivity of *Vibrio cholerae*

Susan M. Butler and Andrew Camilli*

Department of Molecular Biology and Microbiology, Tufts University School of Medicine, 136 Harrison Avenue, Boston, MA 02111

Edited by Howard C. Berg, Harvard University, Cambridge, MA, and approved February 17, 2004 (received for review December 4, 2003)

The role of chemotaxis in the virulence of gastrointestinal pathogens is ill defined. Counterintuitively, nonchemotactic mutants of the polarly flagellated pathogen *Vibrio cholerae* greatly outcompete the wild-type strain during infection of the small intestine. We show that the out-competition phenotype is dependent on the direction of flagellar rotation and independent of Toxin Co-regulated Pilus function. Specifically, the out-competition associated with the loss of chemotaxis required the presence of counterclockwise-biased flagellar rotation and smooth straight runs by the bacteria. In contrast, a nonchemotactic strain with clockwise-biased flagellar rotation was confined to small-scale net movement and was attenuated for infection. The significance of the out-competition phenotype was examined and was shown to correlate with a true increase in infectivity. Counterclockwise-biased mutants are aberrantly distributed throughout the infant mouse small intestine and we find that the expression of virulence factors occurs normally in all segments. Thus, alteration of the chemotactic properties of *V. cholerae* allows it to exploit additional niches in the host intestine.

The Gram-negative bacterium *Vibrio cholerae* is the causative agent of the epidemic disease cholera. Cholera patients are afflicted with a profuse watery diarrhea resulting from the action of the ADP-ribosylating cholera toxin (CT). This organism is highly motile by means of a single polar sheathed flagellum and is believed to use the processes of motility and chemotaxis to travel from the lumen of the small intestine to its preferred intestinal niche on the intestinal epithelium. In this niche *V. cholerae* expresses a number of virulence factors including CT and the toxin co-regulated type IV pilus (TCP). The latter has been shown to be essential for colonization of humans (1), as well as in the infant mouse model of infection (2).

Within the *V. cholerae* genome are multiple paralogues of chemotaxis genes (3). Despite the presence of three chemotaxis operons, only one of these operons is required for chemotaxis (4). The function of the remaining chemotaxis operons remains unknown. Chemotaxis in many organisms is achieved by modulating change in the direction of flagellar rotation from the default direction of counterclockwise (CCW) to clockwise (CW) rotation. In the peritrichously flagellated bacterium *Escherichia coli*, CCW rotation results in the bacterium swimming smoothly in a mostly straight line, whereas CW rotation causes the cell to turn abruptly in a process known as tumbling (5). Because of the presence of a single polar flagellum, *V. cholerae* does not tumble *per se* but instead reverses direction briefly, thereby allowing the bacterium to randomly reorient itself and swim in a new direction.

Although motility and chemotaxis are believed to guide *V. cholerae* to its preferred colonization site within the small intestine, the precise role of each of these processes during infection has not been clearly established. Previous work by Freter *et al.* (6) revealed that motility is required for the establishment of an infection. However, subsequent work by two other groups indicated that motility might in fact be dispensable for infection (7, 8). Much of this prior work was done by using undefined nonmotile mutants, and we have since shown that defined nonmotile mutants of the El Tor biotype, whether flagellated or aflagellated, are severely attenuated in the infant mouse model of infection (9). In contrast to the attenuation seen with nonmotile mutants, the loss of chemotactic ability by itself does not inhibit *V. cholerae* infection. On the contrary, motile but nonchemotactic El Tor biotype *V. cholerae* dramatically outcompete the wild type during infection of the infant mouse (9, 10).

A similar competitive advantage was also seen with fresh cholera stool bacteria. Stool *V. cholerae* (El Tor, Inaba serotype) out-competed *in vitro* grown *V. cholerae* from 10- to 100-fold in the infant mouse small intestine, and this competitive advantage was maintained after incubation of stool bacteria in local pond water for several hours (11). However, this advantage was lost after subsequent growth in LB and was therefore transient. Despite their being motile, transcriptional profiling of stool *V. cholerae* showed repression of all *cheW* and *cheR* paralogues compared with a stool isolate grown *in vitro* (11). In *E. coli* (12) and *V. cholerae* (data not shown), both *cheW* and *cheR* are required for chemotaxis, and mutations in either gene result in a CCW-biased, smooth swimming phenotype. These data suggest that *V. cholerae* exit the human host in a transiently nonchemotactic state. Such a state would augment the infectivity of stool *V. cholerae* in the infant mouse model and possibly aid rapid epidemic spread of cholera in humans.

In this study we have determined that the out-competition phenotype during infection (*in vivo*) requires the presence of a CCW-biased flagellum, because nonchemotactic CW-biased *V. cholerae* were attenuated *in vivo*. In addition, we show that nonchemotactic CCW-biased *V. cholerae* induce virulence gene expression throughout the length of the infant mouse small intestine. Finally, we demonstrate that the out-competition phenotype corresponds with a one-order-of-magnitude decrease in the infectious dose that may have relevance for understanding fecal–oral spread of cholera.

Materials and Methods

Bacterial Strains and Plasmids. *V. cholerae* strains used in this work are derivatives of the El Tor biotype strain C6709-1. All strains and plasmids used in this study are listed in Table 1. Bacterial strains were grown in LB broth with aeration at 37°C or on LB agar plates at 37°C. L agar (without salt) was supplemented with 10% sucrose for counter selection of the pCVD442-*lac* plasmid derivatives. Chemotaxis assays were done in swarm agar (1% tryptone/0.5% NaCl/0.3% agar), and swarm plates were incubated at 37°C overnight. Antibiotics were used at the following concentrations: ampicillin (Ap), 50 $\mu g \cdot ml^{-1}$; kanamycin (Kn),150 $\mu g \cdot ml^{-1}$; streptomycin (Sm), 100 $\mu g \cdot ml^{-1}$; and tetracycline (Tc), 1 and 3 $\mu g \cdot ml^{-1}$.

This paper was submitted directly (Track II) to the PNAS office.

Abbreviations: Ap, ampicillin; CCW, counterclockwise; cfu, colony-forming units; CT, cholera toxin; CW, clockwise; Kn, kanamycin; Sm, streptomycin; Tc, tetracycline; TCP, toxin co-regulated type IV pilus.

*To whom correspondence should be addressed. E-mail: andrew.camilli@tufts.edu.

www.pnas.org/cgi/doi/10.1073/pnas.0308052101

Table 1. Bacterial strains and plasmids used in this study

Strain/plasmid	Relevant genotype (phenotype)	Source/ref.
V. cholerae		
AC-V51	C6709-1, Sm^R (chemotactic [che^+])	34
AC-V66	C6709-1 *lacZ*::*res-tet-res*, Sm^R Tc^R (che^+)	35
AC-V1033	AC-V66 *cheYD60N* (che^-, CCW-biased)	9
AC-V1323	AC-V66 Δ*cheY* (che^-, CCW-biased)	This work
AC-V1035	AC-V1033 *ctxA*::*tnpR*^{mut135} merodiploid, Sm^R Tc^R Ap^R	9
AC-V1036	AC-V1033 *tcpA*::*tnpR*^{mut135} merodiploid, Sm^R Tc^R Ap^R	This work
AC-V1634	AC-V51 Δ*tcpA* (che^+)	This work
AC-V1635	AC-V1033 Δ*tcpA* (che^-, CCW-biased)	This work
AC-V1399	AC-V66 *cheYD16KY109W* (che^-, CW-biased)	This work
AC-V1636	AC-V1399 Reverted to wild-type *cheY* (che^+)	This work
MKW107	O395 (CTX^{calc}-Knϕ), Sm^R Kn^R	20
E. coli		
DH5α*λpir*	F$^-$ Δ(*lacZYA-argF*)U169 *recA1 endA1 hsdR17 supE44 thi-1 gyrA96 relA1 λ*::*pir*	36
SM10*λpir*	*thi recA thr leu tonA lacY supE* RP4–2-Tc::Mu *λ*::*pir*	35
Plasmids		
pCVD442-*lac*	Parent allelic exchange vector	13
pMMB67EH	Low-copy plasmid	37
p*cheY*	pMMB67EH::*cheY*, Ap^R	This work
pSB27	pCVD442-*lac*::Δ*cheY*, Ap^R	This work
pSB29	pCVD442-*lac*::*cheYD16K*, Ap^R	This work
pSB34	pCVD442-*lac*::*cheYY109W*, Ap^R	This work
pSB66	pCVD442-*lac*::Δ*tcpA*, Ap^R	This work
pSB67	pCVD442-*lac*::*cheY*, Ap^R	This work

Strain Constructions. The alleles for construction of deletion and point mutation strains were generated by splicing overlap extension PCR with PFU polymerase (Stratagene). PCR products were cloned into the pCR-Script Amp SK vector (Stratagene). Outer primers contained *Sac*I and *Sph*I restriction sites subsequently used to subclone the fragment into the pCVD442-*lac*. *E. coli* Sm10*λpir* carrying each plasmid were mated with *V. cholerae*. The deletions and point mutations were introduced into the *V. cholerae* genome by allelic exchange with pCVD442-*lac* as described (13). PCR and DNA sequencing were used to confirm the presence of the correct mutations.

Video Tracking. *V. cholerae* strains were observed under ×40 dark-field magnification by using a Zeiss Axioplan 2 microscope. Images of the bacteria were captured by using OPENLAB 3.1.5 (Improvision, Lexington, MA). For each strain a total of 150 bacteria were recorded at 1-s intervals, and the frequency of direction change was calculated as the mean number of direction changes per second.

Complementation Analysis. *cheY* (bases −14 to +435) was amplified by PCR, cloned into PCR-Script Amp SK, and subcloned into the low-copy-number vector pMMB67EH by using *Sac*I and *Sph*I restriction sites incorporated into the primers used for amplification. The complementing plasmid p*cheY* and the pMMB67EH vector were introduced into *V. cholerae* by electroporation. The pMMB67EH vector with and without *cheY* was stable during growth *in vitro* and *in vivo*.

Competition Assays. The competitive index (CI) was determined after intragastric inoculation of 5-day-old CD-1 mice as described (2). Briefly, each mouse was inoculated with ≈10^5 colony-forming units (cfu) of a 1:1 mixture of wild-type ($LacZ^+$) and mutant ($LacZ^-$) overnight cultures. In addition, 2 ml of LB was inoculated with ≈10^4 cfu of this mixture and grown at 37°C overnight. At 24 h postinoculation, animals were euthanized and the small intestines were removed. These were homogenized in LB + 20% glycerol, and serial dilutions were plated on LB agar supplemented with Sm and 40 $\mu g \cdot ml^{-1}$ of 5-bromo-4-chloro-3-indolyl β-D-galactopyranoside (X-Gal). The CI is the ratio of $LacZ^-$ to $LacZ^+$ bacteria after 24 h of infection divided by the ratio of $LacZ^-$ to $LacZ^+$ bacteria after growth overnight in LB.

Intestinal CTXΦ Transduction Assay. This assay was done as described (14). Briefly, 5-day-old mice were inoculated intragastrically with 10^6 cfu of a 1:1 mixture of phage donor (MKW107, $LacZ^+$, Sm^R, Kn^R) and recipient ($LacZ^-$, Sm^R, Tc^R) strain from overnight cultures. At 10 h postinoculation the small intestines were removed, homogenized, and plated on LB agar plus Sm and X-Gal, and LB agar plus Kn and Tc. The frequency of transduction was calculated as the total number of transductants (Kn^R, Tc^R) divided by the total number of recipient cells (Sm^R, $LacZ^-$) in the small intestine.

***In Vivo* Resolution Assays.** Strains harboring *tnpR* fusions (*cheYD60N ctxA*::*tnpR* and *cheYD60N tcpA*::*tnpR*) were grown overnight at 37°C with aeration in LB broth supplemented with Sm, Ap, and Tc. Approximately 10^6 cfu of each strain was inoculated intragastrically into 5-day-old mice. At 7 h postinoculation the small intestine was removed and divided into four segments of equal length. Each segment was homogenized and plated, and the percent Tc^S cfu was calculated as described (14).

Determination of ID_{50}. Five-day-old CD-1 mice were inoculated intragastrically with doses ranging from ≈10 to 10^4 cfu. Small intestines were removed at 24 h, homogenized, and plated to determine the number of cfu per small intestine. The limit of detection was ≈10 cfu, and values equal to or greater than this were recorded as a positive for infection. The ID_{50} was determined graphically by using the curves in Fig. 3.

Results

Loss of CheY Function Leads to an Out-Competition Phenotype *in Vivo*. We had previously shown that the nonchemotactic *cheY-3D60N* (hereafter *cheYD60N*) mutant, in which the conserved phosphorylation site is rendered nonphosphorylatable (15, 16), out-

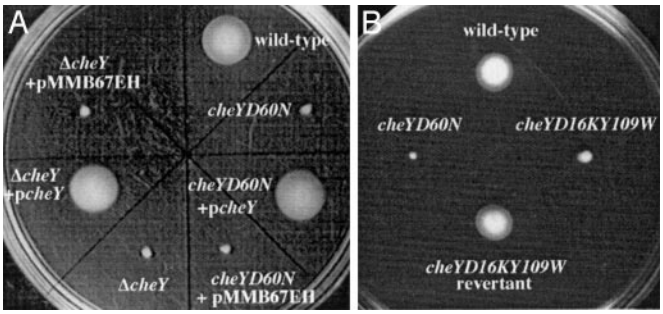

Fig. 1. Analysis of chemotactic ability by using swarm plates. Genetic backgrounds are indicated next to each swarm location.

competes the wild-type strain 70-fold *in vivo* (9). To show that the out-competition phenotype of this strain was not due to an aberrant activity associated with the mutated CheY-3 protein, we constructed an in-frame deletion of *cheY-3* (hereafter *cheY*). The resulting Δ*cheY* strain was defective for chemotaxis as determined in a swarm-plate assay, and this defect was fully complemented by the introduction of the wild-type allele on a low-copy-number plasmid but not by the pMMB67EH vector alone (Fig. 1*A*). The Δ*cheY* strain out-competed the wild-type strain to a similar extent as the *cheYD60N* point mutant when tested *in vivo*, and this out-competition was fully complemented by supply of *cheY* in *trans* (Fig. 2*A*). Thus, it is the lack of CheY function that is responsible for the out-competition phenotype.

Out-Competition Is Independent of TCP. Whereas wild-type *V. cholerae* colonize primarily within the distal half of the infant mouse small intestine, the *cheYD60N* mutant has been shown to be evenly distributed throughout the length of the small intestine

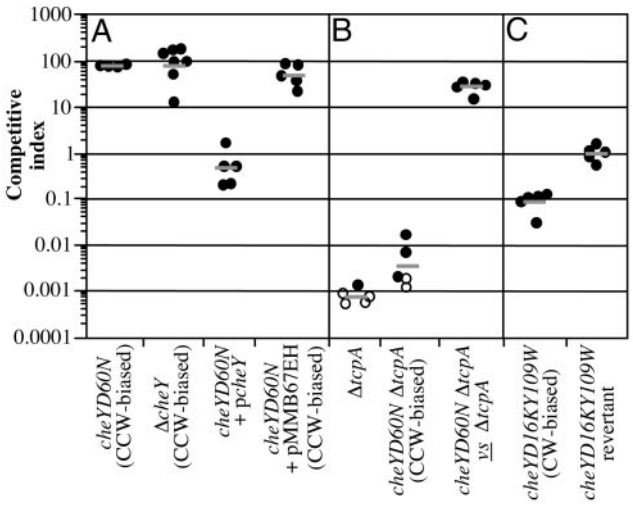

Fig. 2. Competition assays in infant mice between wild-type and mutant *V. cholerae* strains. Mutant strain backgrounds for each experiment are indicated on the *x* axis. Each data point represents the competitive index (CI) from one mouse. The CI is given as the ratio of mutant to wild type after infection divided by the ratio of mutant to wild type after overnight growth in LB. Horizontal bars indicate the geometric mean of the CIs for each experiment. (*A*) Competition between the *cheYD60N*, Δ*cheY*, *cheYD60N* (p*cheY*), and *cheYD60N* (pMMB67EH) strains (all LacZ$^-$) and the wild-type strain (LacZ$^+$). (*B*) Competition between either the *cheYD16KY109W* mutant or *cheYD16KY109W* reversion strain (both LacZ$^-$) and wild type (LacZ$^+$). (*C*) Competition between either the Δ*tcpA* mutant or the *cheYD60N*Δ*tcpA* double mutant and wild type, and between the *cheYD60N*Δ*tcpA* mutant (LacZ$^-$) and the Δ*tcpA* mutant (LacZ$^+$). Open symbols indicate that the mutant was below the limit of detection.

Table 2. Induction of gene expression during infection

Small intestinal segment	Tetracycline-sensitive cfu*, %	
	cheYD60N tcpA::*tnpR*	*cheYD60N ctxA*::*tnpR*
1 (proximal)	93 ± 4	96 ± 2
2	91 ± 3	96 ± 1
3	80 ± 7	96 ± 2
4 (distal)	83 ± 7	89 ± 4

*Induction was measured as percentage tetracycline-sensitive *V. cholerae* cfu recovered at 7 h postinoculation from four segments of equal length spanning the entire infant mouse small intestine. Four mice were infected with each fusion strain, and the mean and standard deviation per segment are shown. The induction of both fusions in the wild-type background at 7 h in the small intestine were previously published; *ctxA*::*tnpR* = 95% (9) and *tcpA*::*tnpR* = 95% (14).

(9). This aberrant distribution is largely responsible for the out-competition phenotype observed with the *cheYD60N* and Δ*cheY* strains. Because TCP is normally required for colonization of the small intestine, we wished to examine whether there are any differences in TCP expression between the wild-type and *cheYD60N* strains *in vivo*. In addition to its requirement for infection, TCP is also the receptor for CTXΦ, the lysogenic bacteriophage whose genome contains the structural genes for CT (17). However, the requirement of TCP for infection is independent of its function as the CTXΦ receptor (18). CTXΦ is secreted from *V. cholerae* via the extracellular protein secretion (EPS) type II secretion system (19), and the expression of TCP can be examined by measuring the frequency of transduction of the kanamycin-resistance-marked derivative CTX^{calc}–KnΦ from a donor strain to the recipient test strain during infection, as described (14, 20). Using this technique, we calculated the frequency of *in vivo* transduction to be 3.3% (±1.0%) for wild-type and 2.5% (±0.7%) for the *cheYD60N* mutant. Thus, there appears to be no gross difference between the two strains with respect to TCP production during infection.

Although TCP production was equivalent between wild-type and *cheYD60N* strains, we wanted to determine whether TCP is expressed by the *cheYD60N* mutant throughout the length of the small intestine. We also wished to examine whether additional virulence genes might be expressed in a similar manner. The *tcpA* gene encodes the pilin subunit of TCP (2), and *ctxA* encodes the enzymatic subunit of CT. We have previously shown that in wild-type *V. cholerae* these genes are fully induced by 7 h postinoculation by using a DNA recombinase (*tnpR*) transcriptional fusion reporter method (14), wherein expression of *tnpR* mediates excision and loss of a tetracycline resistance cassette located elsewhere in the genome. Thus, the level of conversion to tetracycline sensitivity is a direct result of transcriptional induction (for a recent review see ref. 21). Induction of both *tcpA*::*tnpR* and *ctx*::*tnpR* fusions in the *cheYD60N* mutant background was measured at 7 h postinoculation in four divided segments of small intestine (Table 2). The extensive induction of both fusions in the *cheYD60N* mutant observed at 7 h in the distal small intestine was equivalent to induction in the wild-type strain background (9), indicating that the *cheYD60N* mutation and loss of chemotaxis do not affect virulence gene expression at this time point. In addition, both fusions were induced in segments of the proximal small intestine, suggesting that the signals required for TCP and CT expression are present in these locations.

To determine whether nonchemotaxis and TCP act independently to aid colonization, an epistasis test was performed. An in-frame deletion of *tcpA* was constructed in the wild-type and *cheYD60N* mutant backgrounds. Introduction of this mutation in either strain background greatly reduced the level of coloniza-

tion (Fig. 2*B*). However, although the double mutant was attenuated, this attenuation was not as severe as in the single Δ*tcpA* mutant. This was confirmed by competing the *cheYD60N*Δ*tcpA* double mutant against the single Δ*tcpA* mutant (Fig. 2*B*). Although TCP is clearly required for high levels of colonization, the ability of the *cheYD60N*Δ*tcpA* double mutant to out-compete the Δ*tcpA* mutant indicates that chemotaxis and TCP act independently during infection.

CCW-Biased Flagellar Rotation Is Required for Out-Competition. The absence of phosphorylated CheY results in CCW-biased flagellar rotation in *E. coli* and *Salmonella enterica* serovar Typhimurium (22). However, a nonchemotactic state is also observed in the presence of excess levels of CheY-P, which results in CW-biased flagellar rotation (23, 24). We therefore tested whether a CW-biased *V. cholerae* mutant would give rise to the out-competition phenotype during infection. Although CheY has an intrinsic phosphatase activity, it is not adequate for the high turnover of CheY-P required for efficient chemotaxis (25). The protein CheZ stimulates the rate of CheY-P dephosphorylation (26, 27) and is required for chemotaxis in organisms such as *Pseudomonas aeruginosa*, *E. coli*, and *S. enterica* serovar Typhimurium (28, 29). Despite the presence of a single *cheZ* in the *V. cholerae* genome, this gene is not required for chemotaxis in *V. cholerae* (data not shown). We were therefore unable to use the *cheZ* deletion as a CW-biased nonchemotactic test strain. Instead we constructed a *cheYD16KY109W* double point mutant, because the homologous mutations in *E. coli* confer CW-biased flagellar rotation to the bacterium (15, 30, 31). The resulting *V. cholerae cheYD16KY109W* mutant was defective for chemotaxis in swarm agar (Fig. 1*B*).

We confirmed that the *cheYD16KY109W* mutant exhibited CW-biased flagellar rotation by using video tracking to determine the frequency with which the bacteria change their direction of swimming. By using video tracking (32), wild-type *V. cholerae* was calculated to change direction on average once every 7.3 s. In contrast, the *cheYD16KY109W* mutant changed direction on average once every 0.2 s, thus confirming that the double point mutation in *cheY* causes an increased CW-biased flagellar rotation. Finally, the *cheYD60N* mutant changed direction on average only once every 33 s, consistent with CCW-biased flagellar rotation.

In contrast to the *cheYD60N* and Δ*cheY* strains, the *cheYD16KY109W* strain was attenuated *in vivo* (Fig. 2*C*) and had an intestinal distribution similar to that of a nonmotile *V. cholerae* mutant (data not shown). Neither the CCW- nor CW-biased mutant strains showed any competition defect *in vitro*, and both grow with identical kinetics to the wild-type strain during growth in broth culture. The attenuation observed with the *cheYD16KY109W* mutant *in vivo* is in stark contrast to the 70-fold out-competition seen in the presence of CCW-biased flagellar rotation. Expression of TCP in the *cheYD16KY109W* mutant was equivalent to that of the wild-type strain during infection (data not shown), and therefore the attenuation is not a result of a reduction in TCP production. Both the attenuation *in vivo* and the nonchemotactic phenotype were abolished on reversion of the *cheYD16KY109W* mutant to the wild-type sequence by allelic exchange. Complementation analysis could not be performed in this instance because of the dominant negative nature of the D16K mutation (15). Thus, the out-competition phenotype exhibited by *cheY* mutant strains, besides requiring loss of chemotaxis, is critically dependent on the nature of the flagellar rotation and therefore either the net movement capabilities of the bacteria or the mechanical properties of the bacteria as they contact the intestinal mucosa.

CCW-Biased Rotation Results in Increased Infectivity. Although CCW-biased mutants out-compete the wild-type strain *in vivo*, the significance of this out-competition phenotype with respect to virulence has not been established. Early work by Freter *et al.* (6, 10) proposed that the ability of nonchemotactic *V. cholerae* to out-compete wild-type was a result of an inability of the former to enter the intestinal crypts. It was proposed that a large percentage of wild-type *V. cholerae* are killed by innate immune defenses within the crypts and that the out-competition of nonchemotactic *V. cholerae* is a direct result of avoiding such killing. Our results suggest that the ability of nonchemotactic *V. cholerae* to colonize throughout the length of the infant mouse small intestine, as opposed to only the distal portion, may account for the out-competition phenotype. These non-mutually exclusive models could, in either case, manifest in a lower infectious dose for nonchemotactic strains. To examine this, we determined the ID_{50} of the wild-type and *cheYD60N* strains. The ID_{50} of the *cheYD60N* mutant (150 cfu) was approximately one order of magnitude lower than that of the wild-type strain (1,700 cfu) (Fig. 3). The CCW-biased *cheYD60N* mutant is therefore increased for infectivity compared to the wild-type strain.

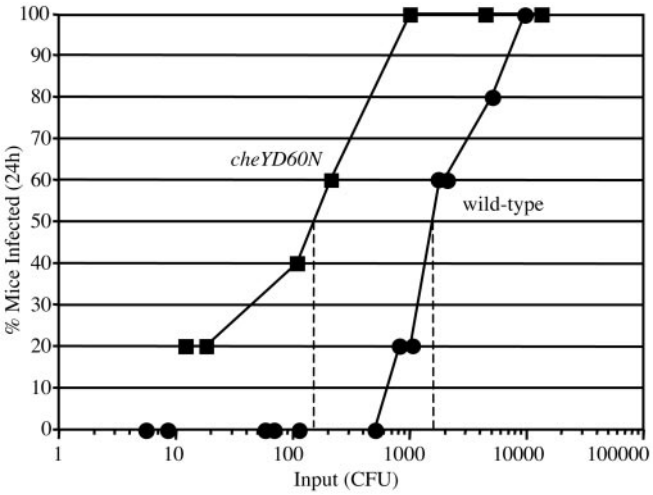

Fig. 3. Determination of the ID_{50} for wild-type and *cheYD60N* strains. Groups of five mice were infected with varying doses (*x* axis) of the wild type (filled circles) or the *cheYD60N* mutant (filled squares). Each data point represents the percentage of the five mice that were infected (*y* axis) after a 24-h period. The limit of detection of the mouse output was 10 cfu per small intestine; however, amongst mouse outputs with detectable numbers of *V. cholerae*, 1,000 cfu was the lowest output observed. The ID_{50} value for each strain was determined graphically.

Discussion

The competitive advantage associated with CCW-biased nonchemotactic *V. cholerae* mutants, as well as the potential existence of a transiently CCW-biased nonchemotactic state in stool *V. cholerae*, makes understanding this out-competition phenotype particularly important. We showed through mutation and complementation analyses that the out-competition phenotype is intricately linked to CCW-biased flagellar rotation, because a CW-biased mutant was attenuated *in vivo*. In addition, we demonstrated the functional independence of TCP and nonchemotaxis in colonization: the former being required for high levels of colonization, but the latter being able to cause an out-competition phenotype even in a TCP-minus strain background. Based on these results, we conclude that it is not the failure to chemotax *per se* that results in the out-competition phenotype but is instead a multifactorial phenomenon requiring motility, expanded host-tissue range in the small intestine, and "head-first" smooth swimming as a result of CCW-biased flagellar rotation.

The aberrant distribution of the *cheYD60N* CCW-biased flagellar rotation mutant throughout the small intestine indicates that it is the process of chemotaxis that is responsible for guiding *in vitro* grown wild-type *V. cholerae* to the distal half of the infant mouse small intestine. Despite this preference, it is apparent that *V. cholerae* in a nonchemotactic CCW-biased state are competent for colonizing sites within the proximal small intestine. The expression of TCP and CT was induced throughout the length of the small intestine in the *cheYD60N* mutant, indicating that signals for induction of virulence gene expression are present throughout and also that the ability of *V. cholerae* to sense and respond to these signals is independent of chemotaxis. Both *cheY* and *cheA* were previously isolated in a screen for *in vivo* regulators of the major virulence gene regulator ToxT (9). Although mutations in both genes resulted in defects with respect to the timing of *ctxA* transcriptional induction, induction of *ctxA* reached wild-type levels by 7 h postinfection. We believe that these genes were identified in our screen because of the delay in induction of virulence gene expression coupled with the competitive advantage associated transposon insertions in these genes.

The propensity of chemotactic *V. cholerae* to colonize mainly the distal portion of the small intestine despite having the ability to colonize throughout suggests that the bacteria are responding to either an unknown chemoattractant or chemorepellent gradient present in the proximal small intestine. Because the small intestine of 5-day-old mice is ≈13 cm in length and because there is unidirectional flow of luminal contents down the small intestine as a result of peristalsis, we believe that such a gradient (whether chemoattractant or chemorepellent) must form between the intestinal epithelium and the lumen, as opposed to over the length of the small intestine. In this model, the concentration of chemoattractant would be higher in the lumen and lower near the epithelium, or *vice versa* in the case of a chemorepellent gradient. In either case, *V. cholerae* would chemotax away from the epithelium and concentrate in the lumen to be transported to the distal small intestine. We have found wild-type *V. cholerae* to be chemotactically attracted to the lining of the proximal small intestine *in vitro* (data not shown). These data suggest that chemorepellents are absent from the surface of the proximal small intestine, and that *V. cholerae* may be responding to a chemoattractant gradient that is higher in the intestinal lumen than at the epithelial surface. If *V. cholerae* is responding to such a gradient in the proximal small intestine, it is likely that the chemoattractants may be nutrients. It is interesting that by the time the intestinal contents reach the distal small intestine, typically the majority of nutrients have been absorbed. This may account for the propensity of *V. cholerae* to colonize the distal small intestine.

Jones *et al.* (33) showed that a CW-biased nonchemotactic mutant of *S. enterica* serovar Typhimurium was defective for adherence to epithelial cells *in vitro* and was attenuated for virulence in a murine infection model. In this case, the resulting unbundled peritrichous flagella are believed to act as a barrier to interaction between the bacterium and the host cell. We also observed an attenuation phenotype for *V. cholerae* with CW-biased flagellar rotation. However, because of the presence of but a single polar flagellum, we do not believe that steric hindrance is the explanation for the attenuation. Instead, we favor the alternative model that the frequent change of direction prevents individual bacteria from making any significant net progress from the lumen to the intestinal wall. This was confirmed by measuring the average distance and paths traveled by individual bacteria over time (Fig. 4*A*). The *V. cholerae* wild-type strain (black lines) and the CCW-biased mutant (dark gray lines) were both found to travel in straight runs an average distance of 39 ± 5 μm in a 1-s interval, whereas the CW-biased mutant (light gray lines) traveled in a zigzag pattern an average distance of only 13 ± 3 μm in 1 s. Taking into account the low-turn frequencies of the wild-type strain and CCW-biased mutant (one turn per 7.3 and 33 s, respectively), and extrapolating the net linear distances traveled over tens of seconds, it is clear that both of these strains are capable of easily traversing the ≈300-μm diameter of the small intestinal lumen of the infant mouse (see cross-section in Fig. 4*B*) to make contact with the intestinal villi. This is in contrast to the CW-biased strain (one turn per 0.2 s), which is confined to a small three-dimensional space within the lumen of the small intestine.

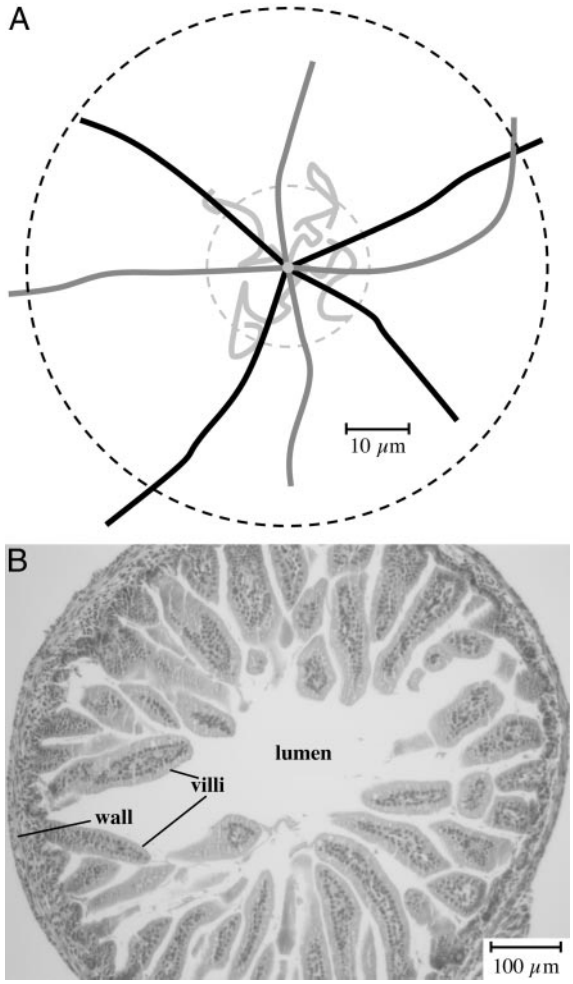

Fig. 4. (*A*) Analysis of net movement by individual *V. cholerae* bacteria. Video images of motile *V. cholerae* were recorded under dark-field microscopy. The net linear distances traveled by individual bacteria over time were calculated, and the means and standard deviations are presented in the text. The mean net linear distance traveled over a 1-s interval by the CW-biased strain is indicated by the inner hatched circle, and that for the wild-type and CCW-biased strains (which were indistinguishable) is indicated by the outer hatched circle. The paths traveled by four representative bacteria of the wild-type (black lines), CCW-biased (dark gray lines), and CW-biased (light gray lines) strains are shown. Note that we have superimposed the original position of each bacterium at the center of the figure and have rotated and distributed the paths to facilitate their visualization. (*B*) Light micrograph (×10 magnification) of a hematoxylin/eosin (H&E)-stained cross section through the small intestine of a 5-day-old mouse. Note that the mucus gel normally overlaying the villi is not present in this micrograph.

These observations may be significant for understanding the chemotactic state and infective potential of stool *V. cholerae*. We have previously shown that *cheW* and *cheR* genes are repressed in stool *V. cholerae*, whereas other essential genes in the chemotaxis signaling pathway, including *cheB* paralogues, are ex-

pressed at levels comparable to that of *in vitro* grown chemotactic *V. cholerae* (11). This combination of gene expression is predicted to lead to an increase in CCW-biased flagellar rotation. In contrast, repression of *cheB* would have been predicted to result in a CW-biased flagellar rotation (12). In support of this model, when observed under a microscope, the motility pattern of stool *V. cholerae* is inconsistent with a CW-biased flagellar rotation state (data not shown). If stool *V. cholerae* have CCW-biased flagellar rotation, then this would explain the hyperinfectivity phenotype previously observed in the infant mouse model of infection (11). That the presence of a CCW-biased nonchemotactic state results in hyperinfectivity is highly unusual given the fact that chemotaxis is required for infection by other organisms such as *Helicobacter pylori*. It is intriguing to speculate that *V. cholerae* has evolved to use a transient CCW-biased nonchemotactic state to increase its infective potential. Whether fresh stool or CCW-biased mutant strains of *V. cholerae* are hyperinfectious in humans remains to be determined.

We thank S. H. Lee for constructing VC1036. This work was supported by National Institutes of Health Grants AI045746 and AI055058.

1. Herrington, D. A., Hall, R. H., Losonsky, G., Mekalanos, J. J., Taylor, R. K. & Levine, M. M. (1988) *J. Exp. Med.* **168,** 1487–1492.
2. Taylor, R. K., Miller, V. L., Furlong, D. B. & Mekalanos, J. J. (1987) *Proc. Natl. Acad. Sci. USA* **84,** 2833–2837.
3. Heidelberg, J. F., Eisen, J. A., Nelson, W. C., Clayton, R. A., Gwinn, M. L., Dodson, R. J., Haft, D. H., Hickey, E. K., Peterson, J. D., Umayam, L., *et al.* (2000) *Nature* **406,** 477–483.
4. Gosink, K. K., Kobayashi, R., Kawagishi, I. & Hase, C. C. (2002) *J. Bacteriol.* **184,** 1767–1771.
5. Eisenbach, M. (1990) *Mol. Microbiol.* **4,** 161–167.
6. Freter, R., O'Brien, P. C. & Macsai, M. S. (1981) *Infect. Immun.* **34,** 234–240.
7. Richardson, K. (1991) *Infect. Immun.* **59,** 2727–2736.
8. Gardel, C. L. & Mekalanos, J. J. (1996) *Infect. Immun.* **64,** 2246–2255.
9. Lee, S. H., Butler, S. M. & Camilli, A. (2001) *Proc. Natl. Acad. Sci. USA* **98,** 6889–6894.
10. Freter, R. & O'Brien, P. C. (1981) *Infect. Immun.* **34,** 222–233.
11. Merrell, D. S., Butler, S. M., Qadri, F., Dolganov, N. A., Alam, A., Cohen, M. B., Calderwood, S. B., Schoolnik, G. K. & Camilli, A. (2002) *Nature* **417,** 642–645.
12. Parkinson, J. S. & Houts, S. E. (1982) *J. Bacteriol.* **151,** 106–113.
13. Donnenberg, M. S. & Kaper, J. B. (1991) *Infect. Immun.* **59,** 4310–4317.
14. Lee, S. H., Hava, D. L., Waldor, M. K. & Camilli, A. (1999) *Cell* **99,** 625–634.
15. Bourret, R. B., Hess, J. F. & Simon, M. I. (1990) *Proc. Natl. Acad. Sci. USA* **87,** 41–45.
16. Sanders, D. A., Gillece-Castro, B. L., Stock, A. M., Burlingame, A. L. & Koshland, D. E., Jr. (1989) *J. Biol. Chem.* **264,** 21770–21778.
17. Waldor, M. K. & Mekalanos, J. J. (1996) *Science* **272,** 1910–1914.
18. Kirn, T. J., Lafferty, M. J., Sandoe, C. M. & Taylor, R. K. (2000) *Mol. Microbiol.* **35,** 896–910.
19. Davis, B. M., Lawson, E. H., Sandkvist, M., Ali, A., Sozhamannan, S. & Waldor, M. K. (2000) *Science* **288,** 333–335.
20. Davis, B. M., Kimsey, H. H., Chang, W. & Waldor, M. K. (1999) *J. Bacteriol.* **181,** 6779–6787.
21. Angelichio, M. J. & Camilli, A. (2002) *Infect. Immun.* **70,** 6518–6523.
22. Eisenbach, M. (1996) *Mol. Microbiol.* **20,** 903–910.
23. Parkinson, J. S. (1978) *J. Bacteriol.* **135,** 45–53.
24. Sanna, M. G., Swanson, R. V., Bourret, R. B. & Simon, M. I. (1995) *Mol. Microbiol.* **15,** 1069–1079.
25. Segall, J. E., Manson, M. D. & Berg, H. C. (1982) *Nature* **296,** 855–857.
26. Hess, J. F., Oosawa, K., Kaplan, N. & Simon, M. I. (1988) *Cell* **53,** 79–87.
27. Sanatinia, H., Kofoid, E. C., Morrison, T. B. & Parkinson, J. S. (1995) *J. Bacteriol.* **177,** 2713–2720.
28. Zhao, R., Collins, E. J., Bourret, R. B. & Silversmith, R. E. (2002) *Nat. Struct. Biol.* **9,** 570–575.
29. Masduki, A., Nakamura, J., Ohga, T., Umezaki, R., Kato, J. & Ohtake, H. (1995) *J. Bacteriol.* **177,** 948–952.
30. Scharf, B. E., Fahrner, K. A., Turner, L. & Berg, H. C. (1998) *Proc. Natl. Acad. Sci. USA* **95,** 201–206.
31. Zhu, X., Amsler, C. D., Volz, K. & Matsumura, P. (1996) *J. Bacteriol.* **178,** 4208–4215.
32. Homma, M., Oota, H., Kojima, S., Kawagishi, I. & Imae, Y. (1996) *Microbiology* **142,** 2777–2783.
33. Jones, B. D., Lee, C. A. & Falkow, S. (1992) *Infect. Immun.* **60,** 2475–2480.
34. Camilli, A., Beattie, D. & Mekalanos, J. (1994) *Proc. Natl. Acad. Sci. USA* **91,** 2634–2638.
35. Camilli, A. & Mekalanos, J. J. (1995) *Mol. Microbiol.* **18,** 671–683.
36. Hanahan, D. (1983) *J. Mol. Biol.* **166,** 557–580.
37. Morales, V. M., Backman, A. & Bagdasarian, M. (1991) *Gene* **97,** 39–47.